



Efficient semianalytical investigation of a fractional model describing human cornea shape

Marwan Abukhaled¹, Yara Abukhaled²

¹Department of Mathematics and Statistics, American University of Sharjah, Sharjah, United Arab Emirates, ²College of Medicine and Health Sciences, Khalifa University, Abu Dhabi, United Arab Emirates

Abstract

Purpose: This study presents a novel application of the semianalytical residual power series method to investigate a one-dimensional fractional anisotropic curvature equation describing the human cornea, the outermost layer of the eye. The fractional boundary value problem, involving the fractional derivative of curvature, poses challenges that conventional methods struggle to address.

Methods: The analytical results are obtained by utilizing the simple and efficient residual power series method. The proposed method is accessible to researchers in all medical fields and is extendable to various models in disease spread and control.

Results: The derived solution is a crucial outcome of this study. Through the application of the proposed method to the corneal shape model, an explicit formula for the curvature profile is obtained. To validate the solution, direct comparisons are made with numerical solutions for the integer case and other analytical solutions available in the literature for the fractional case.

Conclusion: Our findings highlight the potential of the proposed method to significantly contribute to the diagnosis and treatment of various ophthalmological conditions.

Keywords: corneal radius, fractional-order differential equations, nonlinear boundary value problem, semianalytic residual power series

Correspondence: Department of Mathematics and Statistics, American University of Sharjah, Sharjah, United Arab Emirates.

E-mail: mabukhaled@aus.edu

1. Introduction

Mathematical modeling stands as a potent approach in comprehending the kinetics of current intricate phenomena in the realms of physical, biological, and environmental sciences. As a result, researchers are increasingly employing mathematical modeling techniques to garner new insights and facilitate the refinement of system designs and controls.¹⁻⁵

Experimental and theoretical research has concluded that corneal biomechanics relies on geometrical measurements and concrete theories of mechanics, including concepts of equilibrium, geometrical measurements, and complex material behaviors.⁶ For example, Pinsky and Holliday utilized a three-layer corneal geometry with a hydrogel inlay placed under a lamellar flap to describe cellular consumption of oxygen and glucose and production of lactic acid.⁷ Pandolfi and Manganiello studied a numerical model for the human cornea that is able to account for its mechanical behavior in healthy conditions or in the presence of keratoconus under increasing values of intraocular pressure.⁸ Other numerical models in this field include the biomechanics of the human cornea,⁹ and a 3D fluid-solid interaction model of the air-puff test in the human cornea.¹⁰ Additional computational models in several areas of ophthalmology have been presented¹¹⁻¹⁴ as well as in the references therein.

Evidently, accurate corneal modeling plays a critical role in guiding therapeutic and diagnostic interventions for a range of ocular abnormalities, including cataract, glaucoma, and refractive errors. Existing models have encountered challenges in effectively capturing long-range dependencies and achieving sufficient accuracy in corneal shape analysis. This article showcases an effort to overcome this pitfall by considering a fractional model with a simple effective approach to obtain an analytical result to further reflect on the geometric dimensions of the cornea.

Fractional differential equations have gained prominence in recent research, serving as effective tools to model natural phenomena in various fields, including biological systems,^{15,16} infectious diseases,^{17,18} fluid flow,¹⁹ biochemical reactions,²⁰ and control theory.²¹ Due to the inherent nonlocal property of fractional derivative operators, fractional models prove adept at describing memory and hereditary properties of various materials and processes. For example, fractional calculus has been used to model diffusion processes, where the nonlocal property of the fractional derivative reflects the long-range interactions of particles in a medium.²² Additionally, it has been employed in the study of complex systems and signal processing, with the nonlocal property of the fractional derivative adeptly capturing the long-range correlations within the system or signal.²³

While exact solutions to nonlinear fractional-order differential equations remain elusive, numerous numerical and analytical methods, originally designed for integer-derivative differential equations have been adapted to address their fractional-derivative counterparts. Noteworthy among these methods are the fractional Adams-Bashforth-Moulton method,²⁴ the fractional predict-correct method,²⁵ various spectral methods,^{26,27} and artificial network methods.^{28,29} While these meth-

ods demonstrated efficiency and accuracy, they are not without challenges, such as issues of numerical schemes and the necessity to adjust parameters to align with numerical data.³⁰

Among the analytical methods recently applied to solve fractional-derivative equations are the homotopy analysis method,³¹ homotopy perturbation method,³² differential transform method,³³ Green's function-fixed point method,³⁴ and cubic spline method.³⁵ These methods contribute to the expanding toolkit for dealing with the complexities inherent in nonlinear fractional-order differential equations.

The power series method (PSM) is a valuable mathematical technique for solving differential equations, expressing the solution as a series of powers of the independent variable. By directly substituting this power series into the differential equation, a recursive formula for determining the series coefficients is derived. Initially applied to solve fractional differential equations by El-Ajou et al. in 2013,³⁶ the PSM underwent an effective modification in the same year by Abu Arqub,³⁷ resulting in what is known as the residual power series method (RPSM). Distinguished by its capability to present solutions with a desired accuracy through the minimization of residual errors, the RPSM determine coefficients of the truncated series solution via the recursive solution of a system of algebraic equations. This method will be detailed in Section 3.

The remainder of this article is structured as follows: Section 2 summarizes all the theoretical preliminaries. Section 3 delves into the mathematical model of the human cornea, setting the stage for a comprehensive understanding of the subject. Section 4 discusses the existence and uniqueness of the model solution, paving the way for a thorough exploration of the analytical solution presented in Section 5. In this latter section, the effects of parameters on the model will be systematically investigated, contributing to a more nuanced comprehension of the intricate dynamics involved.

2. Preliminaries

This section introduces the fundamental tools of fractional calculus that will be necessary for the remaining parts of this work.

Definition 1. For $m - 1 < \alpha \leq m$, and $m \in \mathbb{N}$, the α^{th} order Riemann-Liouville fractional integral of the real-valued function $f : \mathbb{R}^+ \rightarrow \mathbb{R}$, denoted $J_{t_0}^\alpha f(t)$, is defined by:

$$J_{t_0}^\alpha f(t) = \frac{1}{\Gamma(\alpha)} \int_{t_0}^t (t-s)^{\alpha-1} f(s) ds, \quad \alpha > 0, \quad t > 0. \quad (1)$$

and the α^{th} -order Caputo fractional derivative of $f(t)$, denoted ${}^C D_{t_0}^\alpha$ is defined by:

$${}^C D_{t_0}^\alpha f(t) = J^{m-\alpha} D^m f(t). \quad (2)$$

Henceforth, the Caputo fractional derivative of order α will be denoted D^α

Remark. Based on Definition 1, a more concise expression for $D_{t_0}^\alpha f(t)$ can be stated as:

$$D^\alpha f(t) = \begin{cases} \frac{1}{\Gamma(m-\alpha)} \int_{t_0}^t (t-s)^{m-\alpha-1} f^{(m)}(s) ds, & \text{if } m-1 < \alpha < m \\ f^{(m)}(t), & \text{if } \alpha = m \in \mathbb{N} \end{cases} \quad (3)$$

Remark. The following power rule is a natural consequence of Caputo definition. Let $f(t) = t^p$, $m-1 < \alpha < m$, then:

$$D^\alpha f(t) = \begin{cases} \frac{\Gamma(p+1)}{\Gamma(p-\alpha+1)} t^{p-\alpha}, & \text{if } p > m-1 \\ 0, & \text{if } p \leq m-1 \end{cases} \quad (4)$$

Definition 2. For $0 \leq m-1 < \alpha \leq m$ and $t \geq t_0$, where $m \in \mathbb{N}$, a fractional power series expansion about t_0 for a real valued function $f(t)$ is given by:

$$f(t) = \sum_{n=0}^{\infty} c_n (t-t_0)^{n\alpha}, \quad (5)$$

The proof of the following theorem can be found in Ajou et al.³⁶

Theorem 1. Suppose that $f(t)$ has the power series representation given in Equation (5), where $t_0 \leq t < t_0 + R$, in which R is the radius of convergence. Suppose further that $D_t^{n\alpha} f(t) \in C(t_0, t_0 + R)$, then the coefficients c_n are computed by:

$$c_n = \frac{D_{t_0}^{n\alpha} f(t_0)}{\Gamma(n\alpha + 1)}, \quad (6)$$

where $n = 0, 1, \dots, m+1$.

3. The fractional corneal shape model

As shown in Figure 1,³⁸ the cornea, the slightly raised part of the eyeball, is a transparent dome-shaped structure that envelops the front of the eye. It is the most important refractive surface, accounting for two-thirds of the refractive power of the eye. It is an extremely reactive and sensitive structure as it has more nerve endings than anywhere else in the body. Hence, it is obvious that any change in the corneal structure, radius, or contour can significantly contribute to a set of refractive errors and diseases.³⁹ Additionally, it is important to understand that measurements of corneal parameters can help guide therapeutic and diagnostic purposes. Studies have shown that a microcornea, i.e., a cornea with a small diameter, is usually associated with ocular abnormalities such as cataract formation, iris abnormalities, secondary closed-angle glaucoma, optic nerve hypoplasia, and scleroderma.^{40,41} Microcornea is also associated with Fuchs dystrophy and macular corneal dystrophies.^{40,41}

When it comes to a megalocornea, i.e., a cornea with a large diameter, studies have shown that it is associated with cataract, astigmatism, myopia, and can even progress to lens dislocation and glaucoma later in life.^{40,41} Megalocornea was also noted to be seen in keratoconus as well as lattice and granular dystrophies.^{40,41} When focusing on the radii of the cornea, studies have found that a cornea that is too curved (abnormally small radii) is also found in keratoconus, whereas a cornea that is too flat (large radii) is found in conditions such as cornea plana, a rare bilateral condition associated with severe refractive defects, cataract, and even coloboma.⁴²

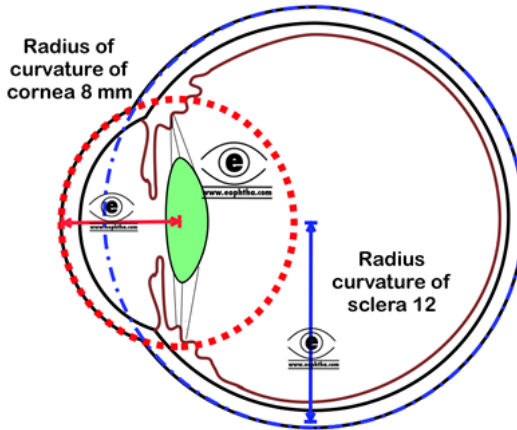


Fig. 1. Radius of corneal curvature.

It is worth noting that several studies highlighted the importance of considering the axial length (AL) and corneal radius of curvature (CRC) as interdependent variables, as the interaction of the two is what helps establish the emmetropization process.⁴³⁻⁴⁵ Hence, expressing them as an AL/CRC ratio is more effective. A study conducted by Iyamu et al. showed that the AL/CRC ratio obtained was 3.16 (SD 0.12) for myopes, 2.95 (SD 0.07) for hyperopes, and 2.96 (SD 0.07) for emmetropes.⁴⁶ This suggests that myopes have a higher AL/CRC ratio than hyperopes and emmetropes. To give another example about the importance of corneal topographers and pachymeters, patient-specific corneal geometry obtained through advanced 3D imaging enables accurate simulation of refractive surgery-induced changes and assessment of postoperative corneal shape and refractive power.⁸ These examples provide concrete proof that understanding corneal geometry parameters can help in categorizing the refractive status and in guiding diagnostic purposes.

The mathematical model describing the corneal shape is given by the nonlinear boundary value problem (BVP):⁴⁷

$$u''(t) - Au(t) + \frac{B}{\sqrt{1 + u'(t)^2}} = 0, \quad (7)$$

subject to Dirichlet boundary conditions (BC):

$$u'(0) = 0, \quad u(1) = 0, \quad (8)$$

where $u(t)$ is a meridian of a surface of revolution describing corneal geometry and the parameters A, B are positive real numbers that are complex in their dependency on various physical and biological factors, including corneal radius.

Various successful attempts to find analytic and numerical approximate solutions to the BVP in Equations (7) and (8) were proposed by some authors. To mention a few, an approximate hyperbolic cosine solution was obtained in Okrasiński et al.,⁴⁷ the perturbation approach was employed in Plociniczak et al.,⁴⁸ Taylor series approach and variational iteration method were discussed in He,⁴⁹ and Green's function-fixed point approach was discussed in Abukhaled et al.⁵⁰ The advantages outlined in the Introduction, given by the nonlocality of the fractional derivative operators, in addition to the fact that Caputo fractional derivative operator is known to preserve the initial and BCs in the fractional counterpart of the integer model, provide a concrete justification for modifying the BVP in Equations (7) and (8) into the following Caputo fractional boundary value problem (FBVP) that models the human corneal topography:

$$D^{2\alpha}u(t) - Au(t) + \frac{B}{\sqrt{1 + (D^\alpha(u(t)))^2}} = 0, \quad (9)$$

where $0 < t < 1$, and $0.5 < \alpha \leq 1$. The BCs remain as given in Equation (8).

4. Existence and uniqueness of the solution

In this section, we provide a sketch of the proof of the existence and uniqueness of the solution to the fractional DE in Equation (9) subject to the BCs in Equation (8). Details of the proof can be found in Erturk et al.⁵¹

Theorem 2. *If $\frac{\max\left\{A, \frac{2\sqrt{3}B}{9}\right\}}{\Gamma(\alpha + 1)} < 1$ then there exists a unique solution to the FBVP in Equation (9) subject to BCs in Equation (8).*

Sketch of the proof

1. The function $f(t) = Au(t) - \frac{B}{\sqrt{1+(D^\alpha u(t))^2}}$ is continuous on $I = [0, 1]$. Let $C(I)$ denote the set of all continuous functions on I , and define \mathcal{B} and $\|u\|_{\mathcal{B}}$ as follows:

$$\mathcal{B} = \{u(t) : u(t) D^\alpha u \in C(I), 0.5 < \alpha \leq 1\}, \text{ and}$$

$$\|u(t)\|_{\mathcal{B}} = \sup_{t \in I} |u(t)| + \sup_{t \in I} |D^\alpha u(t)|.$$

It is straightforward to prove that $(\mathcal{B}, \|\cdot\|_{\mathcal{B}})$ is a Banach space.

2. If $h(t) \in C(I)$ and $0.5 < \alpha \leq 1$, then the fractional BVP:

$$D^{2\alpha}u(t) = h(t), \quad u'(0) = 0, \quad u(1) = 0 \quad (10)$$

has the unique solution:

$$u(t) = \int_0^1 G(t, \xi) h(\xi) d\xi, \quad (11)$$

where:

$$G(t, \xi) = \begin{cases} \frac{(t - \xi)^{2\alpha-1} - (1 - \xi)^{2\alpha-1}}{\Gamma(2\alpha)}, & \text{if } 0 \leq \xi \leq t \leq 1 \\ \frac{-(1 - \xi)^{2\alpha-1}}{\Gamma(2\alpha)}, & \text{if } 0 \leq t \leq \xi \leq 1 \end{cases}. \quad (12)$$

3. The function $u \in \mathcal{B}$ is a solution of the FDE in Equation (9) subject to BCs in Equation (8), provided that u is a solution of the following integral equation:

$$u(t) = \int_0^1 G(t, \xi) \left(Au(\xi) - \frac{B}{\sqrt{1 + (D^\alpha(u(\xi)))^2}} \right) d\xi. \quad (13)$$

4. There exists a positive constant γ such that:

$$Au(t) - \frac{B}{\sqrt{1 + (D^\alpha(u(t)))^2}} \leq A|u(t)| + B|D^\alpha u(t)|^\gamma \quad (14)$$

5. The uniqueness of the solution follows by employing the contraction mapping principle.

5. Residual power series method

In this section, we utilize the RPSM to derive a semianalytic solution to the FBVP in Equation (9) subject to BC in Equation (8). Let $R_u(t)$ be the residual function for Equation (9). Then:

$$R_u(t) = D^{2\alpha}u(t) - Au(t) + \frac{B}{\sqrt{1 + (D^\alpha u(t))^2}}, \quad (15)$$

where $u(t)$ is the fractional power series solution about $t_0 = 0$ of Equation (9) given by:

$$u(t) = \sum_{n=0}^{\infty} c_n \frac{t^{2n\alpha}}{\Gamma(1 + 2n\alpha)}. \quad (16)$$

Here $0.5 \leq \alpha < 1$ and $0 \leq t < r^{\frac{1}{2\alpha}}$, where r is the radius of convergence for the series in (16). Assume that $u(0) = a$, where a will be determined from the BC $u(1) = 0$. By utilizing the BC $u'(0) = 0$, the k^{th} truncated series solution in Equation (16) becomes:

$$u_k(t) = a + \sum_{n=2}^k c_n \frac{t^{2n\alpha}}{\Gamma(1 + 2n\alpha)}. \quad (17)$$

Denoting the corresponding residual function for the approximate solution in Equation (17) by $R_{u_k(t)}$, we obtain:

$$R_{u_k}(t) = D^{2\alpha}u_k(t) - Au_k(t) + \frac{B}{\sqrt{1 + (D^\alpha u_k(t))^2}}. \quad (18)$$

As seen previously,^{35,36} we have $R_u(t) = 0$ and $\lim_{k \rightarrow \infty} R_{u_k}(t) = R_u(t)$ for $0 \leq t < r^{\frac{1}{2\alpha}}$. Since the Caputo fractional derivative of a constant is zero, then $D^{(2\alpha)n}R_u(t) = 0$, and hence:

$$D^{(2\alpha)n}R_{u_k}(0) = D^{(2\alpha)n}R_{u_k}(0), \quad n = 0, 1, \dots, k \quad (19)$$

The determination of the coefficients c_n in the truncated series solution can be obtained by solving the system of algebraic equations generated by:

$$D^{(2\alpha)(k-1)}R_{u_k}(0) = 0, \quad k = 1, 2, \dots \quad (20)$$

6. Results and discussion

We begin by verifying the accuracy of the approximate solution of the FBVP in Equation (9) derived by RPSM against the numerical solution obtained by the fourth-order Runge-Kutta method (RK4) for the integer case $\alpha = 1$ and the parameters $A = B = 1$.

Substituting Equation (17) into Equation (18) gives:

$$R_{u_k} = \sum_{n=2}^k n(n-1)c_n t^{n-2} - \sum_{n=0}^k c_n t^n + \frac{1}{\sqrt{1 + \left(\sum_{n=1}^k n c_n t^{n-1}\right)^2}}. \quad (21)$$

The coefficients $c_n, n = 0, 1, \dots, k$ will be obtained by solving the algebraic system:

$$\frac{d^{k-2}}{dt^{k-2}}R_{u_k} = 0, \quad k = 2, 3, \dots \quad (22)$$

coupled with the implementation of the BCs (8) and the assumption that $u(0) = a$. For example, with $k = m$, Equation (22) will yield $m - 1$ in $m + 1$ unknowns including a , which results from the assumption that $u(0) = a$. The other two equations, in this case, are driven by the BCs $u'(0) = 0$ and $u(1) = 0$, which respectively imply that

$c_1 = 0$ and $a + c_1 + c_2 + \dots + c_m = 0$. For $k = 5, 10,$ and $15,$ the residual power series solution for the integer case were found to be:

$$u_5(t) = 0.3395627 - 0.3302186t^2 - 0.009344162t^4 \tag{23}$$

$$u_{10}(t) = 0.3406783 - 0.3296608t^2 - 0.009359024t^4 - 0.001851326t^6 + 0.0002812365t^8 - 0.00008834878t^{10} \tag{24}$$

$$u_{15}(t) = 0.3406657 - 0.3296671t^2 - 0.009358858t^4 - 0.001851499t^6 + 0.0002813t^8 - 0.0000884t^{10} + 0.0000288t^{12} - 0.00001t^{14} \tag{25}$$

Note that the value of $a,$ assumed for the BC $u(0) = a,$ is the constant term in each of the above approximate series solutions. Figure 2 reflects the high accuracy of the approximate residual power series curve when compared to the fourth-order Runge-Kutta curve for $t \in [0, 1]$ and $\alpha = 1,$ and Table 1 confirms this conclusion.

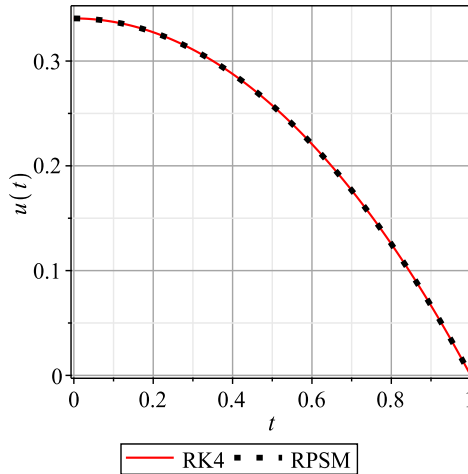


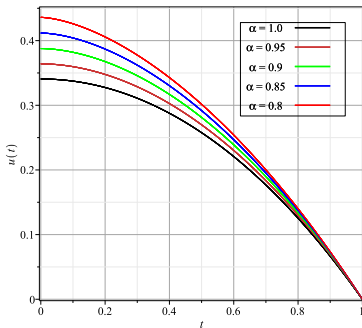
Fig. 2. RK4 curve and 5th-iteration RPSM curve of the FBVP in Equation (9) for the integer case $\alpha = 1$ with $A = 1$ and $B = 1.$

Figure 3 shows the approximate solution obtained by the RPSM for the FBVP in Equation (9) on $[0, 1]$ for the fractional values of $\alpha = 0.95, 0.9, 0.85,$ and 0.8 and $A = B = 1.$ It is inferred that the hereditary property is preserved when comparing these fractional derivative curves with the integer derivative curve ($\alpha = 1.$)

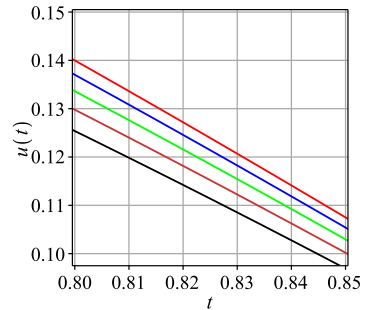
The effect of the parameters A and $B,$ which are related to the radius of the cornea, on the corneal geometry is evident from Figures 3-6. The increase of A and B leads to an increase of the value a representing the initial condition of the surface of revolution describing the corneal geometry.

Table 1. Absolute error for the approximate solution of example 1 for $\alpha = 1$ on the interval $0 \leq t \leq 1$.

t	$u_5(t)$	$u_{10}(t)$	$u_{15}(t)$
0.0	0.001100959	0.000014575	0.000002052
0.1	0.001106561	0.000014547	0.000001962
0.2	0.001122893	0.000014811	0.000002037
0.3	0.001149094	0.000015187	0.000002102
0.4	0.001181340	0.000015648	0.000002127
0.5	0.001209874	0.000016258	0.000002184
0.6	0.001215245	0.000016973	0.000002265
0.7	0.001163618	0.000017564	0.000002325
0.8	0.001001447	0.000017353	0.000002388
0.9	0.000650116	0.000013844	0.000002117
1.0	0	0	0

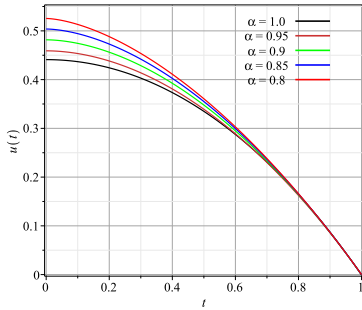


(a) Approximate solution on $[0, 1]$

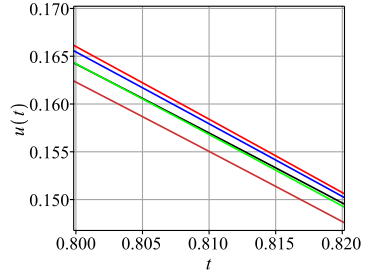


(b) Zoomed approximate solution on $[0.8, 0.85]$

Fig. 3. Approximate RPSM curves of the FBVP in Equation (9) with $A = B = 1$ and various fractional values of α .

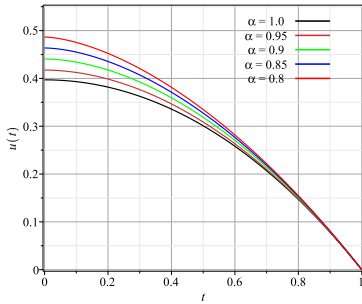


(a)

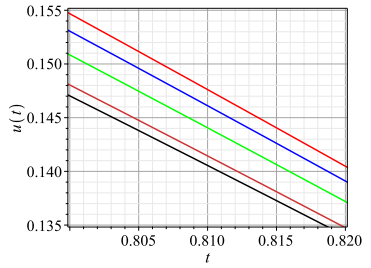


(b)

Fig. 4. Approximate RPSM curves of the FBVP in Equation (9) with $A = 1.72, B = 1.6$ and various fractional order values of α .

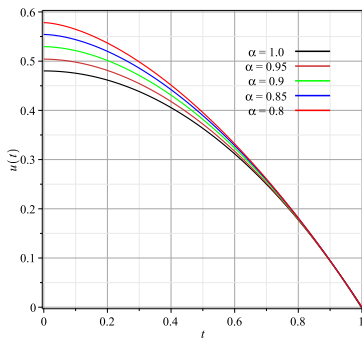


(a)

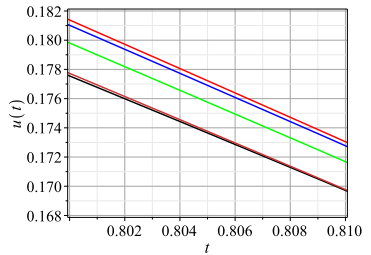


(b)

Fig. 5. Approximate RPSM curves of the FBVP in Equation (9) with $A = 1.38, B = 1.31$ and various fractional order values of α .



(a)



(b)

Fig. 6. Approximate RPSM curves of the FBVP in Equation (9) with $A = 1.6, B = 1.7$ and various fractional order values of α .

7. Conclusion

In this paper, we investigated a mathematical model describing the corneal shape through a Caputo FBVP. Building upon a study presented in Okrasiński et al.,⁴⁷ which derived an integer-order nonlinear BVP assuming radial symmetry for the cross-section of the cornea, we addressed the following two main objectives:

1. Recognizing the importance of considering long-range dependencies in the study of corneal shape, we employed the fractional derivative operator.
2. We utilized the highly accurate and easily implemented fractional RPSM to derive a semianalytic solution.

The derived semianalytic solution provides valuable insights into the influence of corneal parameters on ocular health and disease, offering potential applications in early detection and monitoring.

Overall, our findings underscore the importance of integrating mathematical modeling techniques with clinical practice to enhance our understanding and management of corneal abnormalities.

Declarations

Ethics approval and consent to participate

None required, as this is a review.

Competing interests

None to declare.

Funding

None to declare.

Acknowledgements

None to declare.

References

1. Amiri I, Yupapin P, Rashed A. Mathematical model analysis of dispersion and loss in photonic crystal fibers. *Journal of Optical Communications*, 2023;44, 139–144. doi: 10.1515/joc-2019-0052.
2. Ghasemi P, Goodarzian F, Gunasekaran A, Abraham A. A bi-level mathematical model for logistic management considering the evolutionary game with environmental feedbacks. *The international journal of logistics management*, 2023;34, 1077–1100. doi: 10.1108/ijlm-04-2021-0199.
3. Shanthi R, Devi M, Abukhaled M, Lyons M, Rajendran L. Mathematical modeling of pH-based potentiometric biosensor using Akbari-Ganji method. *International Journal of Electrochemical Science*, 2022;17, 220349. doi: 10.20964/2022.03.48.

4. Abukhaled M, Guessoum N, Alsaedi N. Mathematical modeling of light curves of RHESSI and AGILE terrestrial gamma-ray flashes. *Astrophysics and Space Science*, 2019;364, 1–16. doi: 10.1007/s10509-019-3611-3.
5. Saravanakumar S, Eswari A, Rajendran L, Abukhaled M. A mathematical model of risk factors in HIV/AIDS transmission dynamics: observational study of female sexual network in India. *Appl. Math. Inf. Sci.* 2020;14, 967–976. doi: 10.18576/amis/140603.
6. Pandolfi A. Cornea modelling. *Eye and Vis*, 2020;7(2): doi: 10.1186/s40662-019-0166-x.
7. Pinsky PM, Holliday K. Finite element modeling of metabolic species transport in the cornea with a hydrogel intrastromal inlay. *Invest Ophthalmol Vis Sci*, 2015;56(7): 1131.
8. Pandolfi A, Manganiello F. A model for the human cornea: Constitutive behavior and numerical analysis. *Biomech Model Mechanobiol*, 2006;5(4): 237–246.
9. Montanino A, Gizzi A, Vasta M, Angelillo M, Pandolfi A. Modeling the biomechanics of the human cornea accounting for local variations of the collagen fibril architecture. *ZAMM - Zeitschrift für Angewandte Mathematik und Mechanik*, 2018;98, 2122–2134.
10. Montanino A, Angelillo M, Pandolfi A. A 3D fluid-solid interaction model of the air puff test in the human cornea. *J Mech Behav Biomed Mater*, 2019;94, 22–31.
11. Pinsky PM, Datye DV. A microstructurally-based finite element model of the incised human cornea. *Journal of Biomechanics*, 1991;24(10): 907–922.
12. Pinsky PM, Datye DV. Numerical modeling of radial, astigmatic, and hexagonal keratotomy. *Refractive & Corneal Surgery*, 1992;8(2): 164–172.
13. Pandolfi A, Holzapfel GA. Three-dimensional modeling and computational analysis of the human cornea considering distributed collagen fiber orientation. *Journal of Biomechanical Engineering*, 2008;130(6): 061006. doi: 10.1115/1.2982251.
14. Pandolfi A, Fotia G, Manganiello F. Finite element analysis of laser refractive corneal surgery. *Engineering Computations*, 2009;25, 15–24.
15. Abro K, Atangana A, Gómez-Aguilar J. A comparative analysis of plasma dilution based on fractional integro-differential equation: an application to biological science. *Int J Modell Simul*, 2023;43, 1–10. doi: 10.1080/02286203.2021.2015818.
16. Ali Z, Rabiei F, Hosseini K. A fractal–fractional-order modified Predator–Prey mathematical model with immigrations. *Math Comput Simul*, 2023;207, 466–481. doi: 10.1016/j.matcom.2023.01.006.
17. Azeem M, Farman M, Abukhaled M, Nisar K, Akgul A. Epidemiological analysis of human liver model with fractional operator. *Fractals*, 2023;28, 2340047. doi: 10.1142/s0218348x23400479.
18. Shoaib M, Abukhaled M, Kainat S, Nisar K, Raja M, Zubair G. Integrated Neuro-Evolution-Based Computing Paradigm to Study the COVID-19 Transposition and Severity in Romania and Pakistan. *Int J Comput Intell Syst*, 2022;15, 80. doi: 10.1007/s44196-022-00133-1.
19. Vieru D, Fetecau C, Shah N, Yook S. Unsteady natural convection flow due to fractional thermal transport and symmetric heat source/sink. *Alex Eng J*, 2023;64, 761–770. doi: 10.1016/j.aej.2022.09.027.
20. Rabah F, Abukhaled M, Khuri S. Solution of a complex nonlinear fractional biochemical reaction model. *Math Comput Appl*, 2022;27, 45. doi: 10.3390/mca27030045.
21. Jamil A, Tu W, Ali S, Terrice Y, Guerrero J. Fractional-order PID controllers for temperature control: a review. *Energies*, 2022;15, 3800.
22. Jin B, Rundell W. A tutorial on inverse problems for anomalous diffusion processes. *Inverse Probl*, 2015;31, 035003. doi: 10.1088/0266-5611/31/3/035003.
23. Ortigueira MD, Tenreiro Machado J. Fractional signal processing and applications. *Signal Process*, 2003;83, 2285–2286. doi: 10.1016/s0165-1684(03)00181-6.
24. Zayernouri M, Matzavinos A. Fractional Adams–Bashforth/Moulton methods: an application to the fractional Keller–Segel chemotaxis system. *J Comput Phys*, 2016;317, 1–14. doi: 10.1016/j.jcp.2016.04.041.

25. Zabidi N, Majid Z, Kilicman A, Ibrahim Z. Numerical solution of fractional differential equations with Caputo derivative by using numerical fractional predict–correct technique. *Adv Contin Discrete Models*, 2022;26, 1–23. doi: 10.1186/s13662-022-03697-6.
26. Han C, Wang YL, Li ZY. A high-precision numerical approach to solving space fractional Gray-Scott model. *Appl Math Lett*, 2022;125, 107759. doi: 10.1016/j.aml.2021.107759.
27. Youssri YH, Atta A. Spectral Collocation Approach via Normalized Shifted Jacobi Polynomials for the Nonlinear Lane-Emden Equation with Fractal-Fractional Derivative. *Fractal Fractional*, 2023;7, 133. doi: 10.3390/fractalfract7020133.
28. Shoaib M, Abukhaled M, Kainat S, Nisar KS, Raja MA, Zubair G. Integrated Neuro-Evolution-Based Computing Paradigm to Study the COVID-19 Transposition and Severity in Romania and Pakistan. *International Journal of Computational Intelligence Systems*, 2022;15, 80. doi: 10.1007/s44196-022-00133-1.
29. Weera W, Botmart T, La-inchua T, et al. A stochastic computational scheme for the computer epidemic virus with delay effects. *AIMS Math*, 2023;8, 148–63. doi: 10.3934/math.2023007.
30. Rabah F, Abukhaled M, Khuri S. Solution of a complex nonlinear fractional biochemical reaction model. *Mathematical and Computational Applications*, 2022;27, 45. doi: 10.3390/mca27030045.
31. Qu H, She Z, Liu X. Homotopy Analysis Method for Three Types of Fractional Partial Differential Equations. *Complexity*, 2020;2020, 7232907. doi: 10.1155/2020/7232907.
32. Javeed S, Baleanu D, Waheed A, Shaikat Khan M, Affan H. Analysis of Homotopy Perturbation Method for Solving Fractional Order Differential Equations. *Mathematics*, 2019;7, 40. doi: 10.3390/math7010040.
33. Abukhaled M, Khuri S, Rabah F. Solution of a nonlinear fractional COVID-19 model. *Int J Numer Methods Heat Fluid Flow*, 2022;32, 3657–3670. doi: 10.1108/hff-01-2022-0042.
34. Abukhaled M, Khuri S. RLC electric circuit model of fractional order: a Green's function approach. *Int J Comput Math*, 2023; doi: 10.1080/00207160.2023.2203787.
35. Abu Arqub O, Tayebi S, Momani S, Abukhaled M. Adaptation of the Novel Cubic B-Spline Algorithm for Dealing with Conformable Systems of Differential Boundary Value Problems concerning Two Points and Two Fractional Parameters. *J Funct Spaces*, 2023; 5322092. doi: 10.1155/2023/5322092.
36. El-Ajou A, Abu Arqub O, Al Zhou Z, Momani S. New results on fractional power series: theories and applications. *Entropy*, 2013;15, 5305–5323. doi: 10.3390/e15125305.
37. Abu Arqub O. Application of residual power series method for the solution of time-fractional Schrödinger equations in one-dimensional space. *Fundamenta Informaticae*, 2019;166, 87–110. doi: 10.3233/fi-2019-1795.
38. Majumder P. Anatomy of cornea. (Accessed 14 December 2023). Available from: <https://www.eophtha.com/posts/anatomy-of-cornea>.
39. Grosvenor T. *Primary Care Optometry*. 5th ed. Butterworth-Heinemann, 2007; 22–302.
40. O'Hara M. *Clinical Ophthalmology: A Systemic Approach*. 5th ed. Butterworth-Heinemann, 2004;
41. Seitz B, Langenbucher A, Zagrada D, Budde W, Kus M. Corneal dimensions in patients with various types of corneal dystrophies and their impact on penetrating keratoplasty. *Klin Monatsbl Augenheilkd*, 2000;217, 152–158. doi: 10.1055/S-2000-10338.
42. Denniston A, Murray P. *Oxford Handbook of Ophthalmology*. 2nd ed. Oxford University Press, 2009;
43. Troilo D. Neonatal eye growth and emmetropization—a literature review. *Eye*, 1992;6(2): 154–160. doi: 10.1038/eye.1992.31.
44. Grosvenor T, Scott R. Role of the axial length/corneal radius ratio in determining the refractive state of the eye. *Optometry and Vision Science*, 1994;71(9): 573–579. doi: 10.1097/00006324-199409000-00005.
45. Waltman SR, Hart MW. The cornea. in *Adler's Physiology of the Eye-Clinical Application*. 8th ed. CV Mosby Coy, USA, 1987; 36–59.

46. Iyamu E, Iyamu J, Obiakor C. The role of axial length-corneal radius of curvature ratio in refractive state categorization in a Nigerian population. *International Scholarly Research Notices*, 2011; doi: 10.5402/2011/138941.
47. Okrański W, Plociniczak L. A nonlinear mathematical model of the corneal shape. *Nonlinear Anal. Real World Appl.* 2012;13, 1498–1505. doi: 0.1016/j.nonrwa.2011.11.014.
48. Plociniczak L, Okrański W, Nieto JJ, Domínguez O. On a nonlinear boundary value problem modeling corneal shape. *J. Math. Anal. Appl.* 2014;414, 461–471. doi: 10.1016/j.jmaa.2014.01.010.
49. He J. A remark on "A nonlinear mathematical model of the corneal shape". *Nonlinear Anal. Real World Appl.* 2012;13, 2863–2865. doi: 10.1016/j.nonrwa.2012.04.014.
50. Abukhaled M, Khuri S. An Efficient Semi-Analytical Solution of a One-Dimensional Curvature Equation that Describes the Human Corneal Shape. *Math. Comput. Appl.* 2019;24(8): doi: 10.3390/mca24010008.
51. Erturk V, Ahmadkhanlu A, Pushpendra K, Govidaraj V. Some novel mathematical analysis on a corneal shape model by using Caputo fractional derivative. *Optik*, 2022;261, 169086. doi: 10.1016/j.ijleo.2022.169086.